Available online at www.sciencedirect.com
SCIENCE DIRECT®
Biochemical and Biophysical Research Communications 337 (2005) 281–288
BBRC
www.elsevier.com/locate/ybbrc

Identification of endogenous surrogate ligands for human $P2Y_{12}$ receptors by in silico and in vitro methods ☆

Yosuke Nonaka, Takeshi Hiramoto [1], Norihisa Fujita *

Laboratory of Pharmcoinformatics, Department of Bioinformatics, Ritsumeikan University, Kusatsu, Shiga 525-8577, Japan

Received 16 August 2005
Available online 19 September 2005

Abstract

Endogenous ligands acting on a human $P2Y_{12}$ receptor, one of the G-protein coupled receptors, were searched by in silico screening against our own database, which contains more than 500 animal metabolites. The in silico screening using the docking software AutoDock resulted in selection of cysteinylleukotrienes (CysLTs) and 5-phosphoribosyl 1-pyrophosphate (PRPP), with high free energy changes, in addition to the known $P2Y_{12}$ ligands such as 2MeSADP and ADP. These candidates were subjected to an in vitro Ca^{2+} assay using the CHO cells stably expressing $P2Y_{12}$–$G_{16}\alpha$ fusion proteins. We found that CysLTE4 and PRPP acted on the $P2Y_{12}$ receptor as agonists with the EC_{50} values of 1.3 and 7.8 nM, respectively. Furthermore, we analyzed the phylogenetic relationship of the P2Y, P2Y-like, and CysLT receptors based on sequence alignment followed by evolutionary analyses. The analyses showed that the $P2Y_{12}$, $P2Y_{13}$, $P2Y_{14}$, GPR87, CysLT-1, and CysLT-2 receptors formed a P2Y-related receptor subfamily with common sequence motifs in the transmembrane regions.

Keywords: P2Y receptor; 5-phosphoribosyl 3-pyrophosphate; Cysteinylleukotriene E4; In silico screening; 3D model of GPCR; $G_{16}\alpha$-mediated Ca^{2+} response

In October 2004, the international human genome project reported that approximately 22,000 genes exist on the human genome and about 30% of these genes encode membrane proteins [1,2]. In the post-genome project, the elucidation of the structures of membrane proteins and their functions are urgent issues, since membrane proteins play pivotal roles in the neuronal systems, immune systems, cell differentiation, and so on. Moreover, it has been reported that more than 50% of contemporary medicines act on the membrane proteins such as G-protein coupled receptors (GPCRs) [3].

In the study of molecular-based protein–ligand interaction, a computer plays an important role. For instance, the molecular dynamics (MD) calculation is indispensable to find an energetically stabilized structure of a target protein. The binding site of a ligand on a protein can be identified by a computational docking study. These in silico studies can analyze the 3D structure of the protein–ligand complex and propose ligands that can interact with the target protein [4]. However, the in silico study is difficult to apply on a membrane protein such as a GPCR, because as with nearly all of these membrane proteins, very little of the 3D structure has been elucidated.

In our laboratory, we have obtained practical results in discovering surrogate $P2Y_1$ ligands [5,6] using AutoDock, the docking program developed by Morris et al. [7]. The features of this program are that: (i) a large configuration space can be searched, (ii) the perfect flexibility of a ligand molecule can be taken into consideration, and (iii) docking is accelerated by calculating the interaction between a protein and a ligand in a grid base. The screening system in our laboratory is fully automated and can run three independent programs required for the screening. Our database

☆ This study was partially supported by the Grant-in-Aid for scientific research from Japanese Ministry of Education, Culture, Sports, Science and Technology.
* Correspondent author. Fax: +81 77 561 5203.
E-mail address: nori@is.ritsumei.ac.jp (N. Fujita).
[1] Present address: Department of Pharmacology, National Defense Medical College, Tokorozawa, Saitama 359-8513, Japan.

0006-291X/$ - see front matter © 2005 Elsevier Inc. All rights reserved.
doi:10.1016/j.bbrc.2005.09.052

of animal metabolites was based on the KEGG Ligand Database [8] and the structure of each compound is constructed by energy minimization using the InsightII/CHARMm. Moreover, known P2Y receptor agonists and antagonists are added to this database as an internal marker for the screening. Using these tools, we found the surrogate ligands that bind on the human $P2Y_1$ receptor with high affinity [5].

As for the P2Y receptor belonging to a GPCR family, eight kinds of subclasses, $P2Y_1$, $P2Y_2$, $P2Y_4$, $P2Y_6$, $P2Y_{11}$, $P2Y_{12}$, $P2Y_{13}$, and $P2Y_{14}$, have been classified by human cDNA analyses and functional assays [9]. In addition to these P2Y receptors, two orphan GPCRs, GPR87 and GPR91, have been proposed to be P2Y-like receptors, based on human genome analyses [10]. In order to understand the physiological functions and molecular basis of receptor-related diseases, identification of endogenous ligands for P2Y and P2Y-like receptors is indispensable.

Among the known P2Y ligands, ADP is well established as an important factor for platelet aggregation. Angiostasis is achieved by the activation of blood platelets and the activation is triggered by the specific binding of ADP to the $P2Y_1$ and $P2Y_{12}$ receptors [11,12]. The activation of $P2Y_1$ receptors induces the platelet shape changes and the activation of the $P2Y_{12}$ receptor stabilizes platelet aggregation [13]. In addition to nucleotides, eicosanoids are also known to be profoundly related to the process of thrombosis [14]. Thromboxanes and leukotrienes are biosynthesized from arachidonic acid in almost all cells except for erythrocytes [15]. Thromboxane A2 (TxA2) induces platelet activation, and CysLTs accelerate the platelet aggregation [17]. Although the detailed process is not yet elucidated, the formation and stabilization of platelet plugs are performed very efficiently through the activation of both $P2Y_1$ and $P2Y_{12}$ receptors on platelets.

In the present study, we investigated the molecular targets of the $P2Y_{12}$ receptor using in silico and in vitro methods, and we found that PRPP and CysLTE4 activated the $P2Y_{12}$ receptors. Moreover, we demonstrated that three $P2Y_n$, GPR87, and two CysLT receptors formed a receptor subfamily with common sequence motifs.

Methods

In silico screening. We used the AutoDock 3.0, a ligand flexible docking program [7], according to the manufacturer's instructions with our in-house database. The number of grid points in the *x*-, *y*-, *z*-axis was $60 \times 60 \times 60$ with grid points separated by 0.375 Å. The population size was set to 50. Each docking experiment consisted of a series of 200 simulations. The resulting initial set of 200 receptor–ligand configurations included crude configurations and required further refinement. To this end, the top 10 configurations of binding energy as ranked by AutoDock were 1000 step energy minimized with CHARMm force field in a standard condition. These energy minimizations were calculated using the InsightII/CHARMm programs (Accelrys, San Diego, CA, USA), and the lowest-energy configuration was selected. A total of more than 500 compounds in our database were calculated as ligands by this method. Our 3D compound database was based on the 2D molecules in the KEGG Ligand database (http://www.genome.ad.jp/ligand/). These 2D molecules were converted to 3D and energy minimized using the InsightII/CHARMm programs.

Construction of the $P2Y_{12}$ receptor to a 3D structure. The 3D structure of the $P2Y_{12}$ receptor was constructed on the basis of the coordinates and the conformation of the 3D model of the $P2Y_1$ receptor was constructed by both Fourier transform analysis and homology modeling using the bovine rhodopsin structure as a template [6]. The transmembrane regions (TM) of the $P2Y_{12}$ receptor were determined by alignment with those of the P2Y receptors and bovine rhodopsin. We estimated the following seven transmembrane regions; 29–52aa/TM1, 60–85/TM2, 93–122/TM3, 144–162/TM4, 189–212/TM5, 238–263/TM6, and 276–300/TM7. The amino acids of transmembrane domains on the 3D structure of the $P2Y_1$ receptor were replaced by those of the $P2Y_{12}$ receptor. Additionally, high temperature MD calculation was performed for energy minimization. The conditions of MD calculation were as follows. The InsightII/CHARMm parameter was used. α-Carbon of a principal chain was restrained with the harmonic function ($k = 1$ kcal/mol Å^2) so that the structural change with radical tertiary structure might not be caused [6].

Cell culture and generation of stably transfected cell lines. The $hP2Y_1$–$G_{16}\alpha$, $hP2Y_{12}$–$hG_i\alpha$ and $hP2Y_{12}$–$hG_{16}\alpha$ fusion genes was generated by a two-step PCR protocol using KOD DNA polymerase (TOYOBO, Osaka). Each gene was cloned into the Flp-In System expression vector, pcDNA5/FRT (Invitrogen, Carlsbad) [5]. The accuracy of all PCR-derived sequences was confirmed by DNA sequence analyses using the ABI PRISM 3100 Genetic Analyzer (Applied Biosystem, Foster City). The cDNA coding $hG_{16}\alpha$ in pCIS plasmid was kindly provided by Prof. Haga in Gakushuin University.

CHO-K1 (Chinese hamster ovary) cell line was used to generate Flp-In CHO cell line (Invitrogen). Flp-In CHO cells were maintained in Ham's F-12 Medium (Invitrogen) supplemented with 100 U/ml penicillin, 100 μg/ml streptomycin, 100 μg/ml zeocin, 2 mM L-glutamine, and 10% fetal bovine serum at 37 °C in a CO_2 incubator with 5% CO_2.

Purified plasmid DNA (1 μg) containing the $hP2Y_{12}$–$hG_{16}\alpha$, $hP2Y_1$–$hG_{16}\alpha$ or $hP2Y_{12}$–$hG_i\alpha$ genes were transfected into Flp-In CHO cells using Lipofectamine 2000 (Invitrogen). After transfection, cell populations stably expressing these genes were obtained by selection with 0.5 mg/ml hygromycin B (Invitrogen). Clonal cell lines were isolated, and the expression of $hP2Y_{12}$–$hG_{16}\alpha$, $hP2Y_1$–$hG_{16}\alpha$ or $hP2Y_{12}$–$hG_i\alpha$ fusion proteins was confirmed by RT-PCR method and Western blot analysis. We used the previously prepared cell line expressing the $hP2Y_1$–$hG_q\alpha$ fusion receptors [5].

Measurement of intracellular Ca^{2+} concentration. The intracellular Ca^{2+} concentration ($[Ca^{2+}]_i$) was measured using Ca^{2+} indicator Fura-2/AM (Calbiochem, San Diego) in CHO cells perfused with a standard bath solution consisting of Krebs–Ringer bicarbonate Hepes buffer supplemented with 5.6 mM glucose and 0.05% BSA. Fura-2-loaded cells were transferred to the recording chamber mounted on the stage of an inverted microscope (Olympus IX70, Tokyo). The recording chamber was maintained at 37 °C and was perfused continuously at a rate of 1.5 ml/min. All nucleotides or nucleotide analogues used were from Sigma. The measurement of $[Ca^{2+}]_i$ was performed by fluorescence changes at 340 and 380 nm, and the fluorescence intensities were analyzed using Meta-Fluor version 6.1 (Universal Imaging, Downingtown).

Phylogenetic analyses. Phylogenetic analysis can embody the evolutional relationship based on the similarity of the primary sequence in the alignment of proteins. In this research, the alignment was calculated by ClustalX (http://www.biolinux.org/clustalx.html), and uncertain portions, such as gaps, were deleted from BioEdit. With this alignment, more precise phylogenetic analysis was conducted by neighbor joining with 1000 bootstrap steps (MEGA2) [18].

In this research, 169 amino acid sequences of GPCRs (38 amine receptors, 18 P1 and $P2Y_n$ receptors), three leukotriene receptors, seven hormone receptors, five opsin receptors, seven prostaglandin receptors, 17 chemokine receptors, and 74 other peptide receptors were retrieved from the NCBI Reference Sequence database and used for phylogenetic analysis. In addition, nine sequences of orphan GPCRs similar to those of the $P2Y_n$ receptors were retrieved and added.

Results

The effects of the $P2Y_1$ agonists and antagonists on the expressed receptor were measured using the cells stably expressing $P2Y_1$ fusion receptors. First, the influences were investigated for 2-methylthio ADP (2MeSADP), which is a known $P2Y_1$ agonist, on the $[Ca^{2+}]_i$ of $hP2Y_1$–$hG_q\alpha$ and $hP2Y_1$–$hG_{16}\alpha$ cells (Fig. 1, upper). The results showed that 2MeSADP induced the $[Ca^{2+}]_i$ increases in both of the cells with dose dependency. The EC_{50} values of 2MeSADP for the $hP2Y_1$–$G_q\alpha$ and $hP2Y_1$–$hG_{16}\alpha$ receptors were 0.16 and 0.06 nM, respectively. On the other hand, the EC_{50} value obtained from the wild type cells that express a small amount of $P2Y_1$ receptors [19] was 4.8 nM. Furthermore, in the presence of 10 μM PPADS, which is a known $P2Y_1$ antagonist, the increase in the $[Ca^{2+}]_i$ by 1 nM 2MeSADP was completely inhibited.

The effects of $P2Y_{12}$ agonist and antagonist were also examined using the cells stably expressing $P2Y_{12}$ fusion receptors. First, the influence of 2MeSADP, a known $P2Y_{12}$ agonist, on the $[Ca^{2+}]_i$ of the $hP2Y_{12}$–$G_i\alpha$ and $hP2Y_{12}$–$hG_{16}\alpha$ cells was investigated (Fig. 1, bottom). As a result, 2MeSADP stimulated the $[Ca^{2+}]_i$ increase in the $hP2Y_{12}$–$hG_{16}\alpha$ cells in a high affinity manner, with an EC_{50} value of 0.059 nM. Furthermore, 10 μM 2MeSAMP, a known $P2Y_{12}$ antagonist, inhibited the 1 nM 2MeSADP-induced $[Ca^{2+}]_i$ increase. In contrast, the dose–response curve of 2MeSADP obtained in the $[Ca^{2+}]_i$ change of the

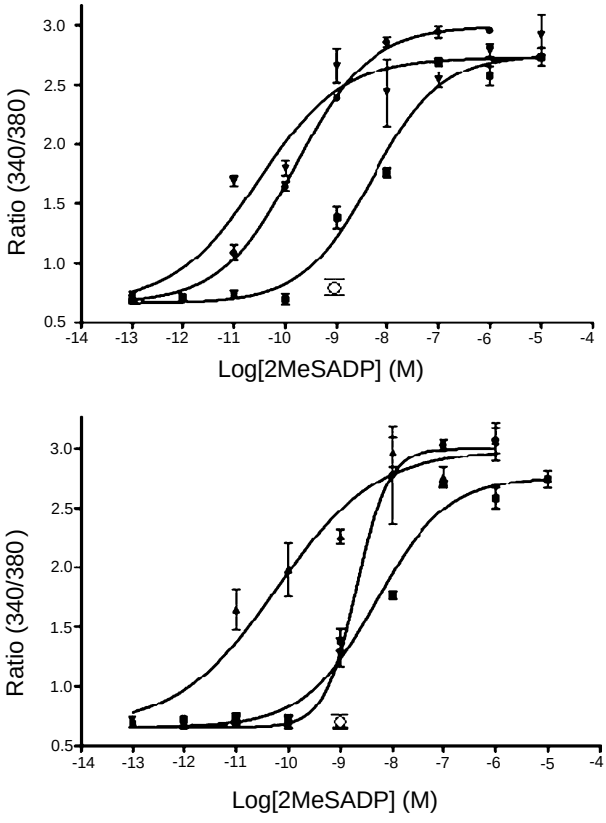

Fig. 1. Dose–response curves for 2MeSADP-evoked $[Ca^{2+}]_i$ increases via the expressed hP2Y–hGα fusion proteins. (Upper) The results from $hP2Y_1$–hGα fusion proteins. Wild-type CHO cells (■) and cells stably expressing $hP2Y_1$–$hG_q\alpha$ (●), and $hP2Y_1$–$hG_{16}\alpha$ (▼) were used. Open circle represents the result in the $hP2Y_1$–$hG_{16}\alpha$ cells in the presence of 10 μM PPADS. (Bottom) The results from $hP2Y_{12}$–hGα fusion proteins. Wild-type CHO cells (■) and cells stably expressing $hP2Y_{12}$–$hG_{16}\alpha$ (▲) and $hP2Y_{12}$–$hG_i\alpha$ (●) fusion proteins were used. Open circle represents the result in the $hP2Y_{12}$–$hG_{16}\alpha$ cells in the presence of 10 μM 2MSAMP. Individual curves represent means ± SEM of three to five experiments each measuring at least 10 single cells.

Table 1
The results of the in silico screening using the AutoDock program

	Ligand	δG
1	Leukotriene F4	−13.73
2	Chenodeoxycholic acid	−12.39
3	Adenosine-4P	−12.36
4	Solanidine	−12.29
5	Leukotriene E4	−12.27
6	ITP	−12.23
7	Leukotriene D4	−12.22
8	Prostaglandin E3	−12.16
9	Docosahexaenoic acid	−12.03
10	Geranylgeranyl diphosphate	−11.93
11	Eicosapentanoic acid	−11.76
12	Cholesterol	−11.75
13	XTP	−11.67
14	Leukotriene A4	−11.64
15	Ergosterol	−11.61
16	Heroin	−11.56
17	2MeSADP	−11.28
18	Ecdysone	−11.28
19	Cholic acid	−11.22
20	Arachidonic acid	−11.13
21	Deoxycholic acid	−11.13
22	TRH	−11.09
23	XDP	−11.08
24	Icosanoic acid	−11.07
25	Retinol	−11.05
26	IDP	−11.03
27	Leukotriene B4	−11.03
28	Ajmaline	−10.99
29	ATPγS	−10.93
30	Morphine	−10.92
31	Prostaglandin A1	−10.67
32	*S*-Adenosylmethionin-amine	−10.67
33	ADP-glu-ADP-2P	−10.61
34	Stearic acid	−10.57
35	GTP	−10.54
36	ADP	−10.51
37	Codeine	−10.51
38	UDP-glucose	−10.5
39	ATP	−10.42
40	UDP	−10.42
41	Elaidic acid	−10.34
42	CTP	−10.33
43	PRPP	−10.27
44	Cortisol	−10.27
45	UTP	−10.31
46	IDP	−10.26
47	Cinochonine	−10.18
48	IMP	−10.15
49	CDP	−10.01
50	A3P5PS	−9.99

The top 50 compounds according to the AutoDock binding energy (kcal/mol) are listed. Dopamine was the highest in amine compounds with the energy change of −6.83.

$hP2Y_{12}$–$hG_i\alpha$ cells was not significantly different from that of the wild type cells. The EC_{50} values were 2.0 and 4.7 nM, respectively.

As previously reported, we have searched for $P2Y_1$ ligands using in silico screening with the 3D model of $P2Y_1$ receptor [5]. In the present study, we also performed in silico screening for $P2Y_{12}$ receptor ligands using similar methods. Subsequently, in addition to the known $P2Y_{12}$ ligands such as 2MeSADP and some nucleotides, CysLTs, arachidonic acid derivatives, and PRPP, a ribose metabolite, were selected in the top 50 (Table 1). In the previous report, we showed that PRPP activated the $P2Y_1$ receptors with an EC_{50} value of 15 nM and predicted that PRPP had an agonistic effect on the $P2Y_{12}$ receptor. Therefore, the influence of PRPP on the $[Ca^{2+}]_i$ of $hP2Y_{12}$–$hG_{16}\alpha$ and $hP2Y_1$–$hG_{16}\alpha$ cells was investigated. Consequently, PRPP increased the $[Ca^{2+}]_i$ in the wild type cells with the EC_{50} value of 530 nM, while in the $hP2Y_{12}$–$hG_{16}\alpha$ and $hP2Y_1$–$G_{16}\alpha$ cells, the EC_{50} values were 7.8 and 4.6 nM, respectively (Fig. 2, upper). The PRPP-induced $[Ca^{2+}]_i$ increase in the $hP2Y_{12}$–$hG_{16}\alpha$ cells was inhibited by the $P2Y_{12}$ antagonist, 10 μM 2MeSAMP (Fig. 2, bottom).

As presented in Table 1, several leukotrienes were selected by the in silico screening for the $P2Y_{12}$ receptors. The $[Ca^{2+}]_i$ assay with the $hP2Y_{12}$–$hG_{16}\alpha$ expressing cells was performed to verify in vitro activity of these candidates. The assay results clearly showed that CysLTE4 activated the $hP2Y_{12}$ receptors with an EC_{50} value of 1.3 nM. Furthermore, 10 μM 2MeSAMP completely inhibited the 10 nM CysLTE4-induced $[Ca^{2+}]_i$ increase (Fig. 3). The wild type CHO cells did not show any response to 1 μM CysLTE4 (data not shown).

The structures of $P2Y_{12}$ receptor–ligand complexes were constructed by using Insight II, and energy minimizations were conducted to produce stable 3D structures. 1-diphosphoric acid of PRPP was shown to interact with Glu263 of TM6, and the ribose portion interacts with Ser101 of TM3, and 5-phosphoric acid portion interacts with Glu281 and Leu284 of TM7. Thus, the interactions of the phosphoric acid portions were carried out by TM6 and TM7, and

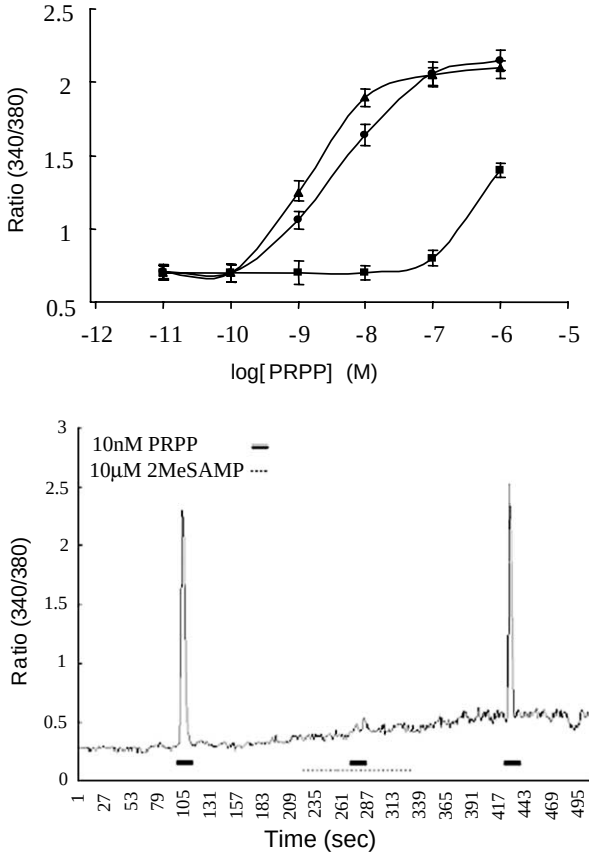

Fig. 2. Dose–response curves for PRPP-evoked $[Ca^{2+}]_i$ increases via the expressed hP2Y–hGα fusion proteins. (Upper) Wild-type CHO cells (WT: ■) and CHO cells stably expressing $hP2Y_1$–$hG_{16}\alpha$ ($P2Y_1$–G_{16}: ▲) and $hP2Y_{12}$–$hG_{16}\alpha$ ($P2Y_{12}$–$G_{16}\alpha$: ●) fusion proteins were used. Individual curves represent means ± SEM of three to five experiments each measuring at least 10 single cells. (Bottom) Antagonistic effect of 2MeSAMP on the 10 nM PRPP-evoked $[Ca^{2+}]_i$ increases via the $P2Y_{12}$ fusion receptors in the presence or absence of 10 μM 2MeSAMP.

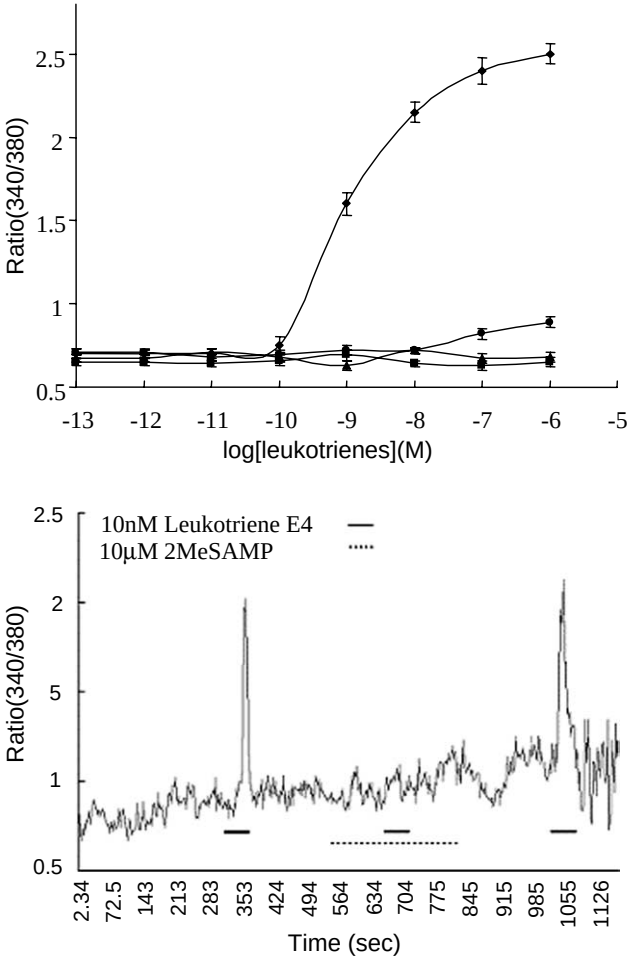

Fig. 3. Dose–response curves for leukotriene-evoked $[Ca^{2+}]_i$ increases via the expressed $hP2Y_{12}$–$hG_{16}\alpha$ fusion proteins. (Upper) $hP2Y_{12}$–$hG_{16}\alpha$ cells were stimulated by CysLT-F4 (▲), -B4 (■), -E4 (♦) or -D4 (●). (Bottom) Antagonistic effects of 2MeSAMP on the 10 nM CysLTE4-evoked $[Ca^{2+}]_i$ increases in the presence or absence of 10 μM 2MeSAMP.

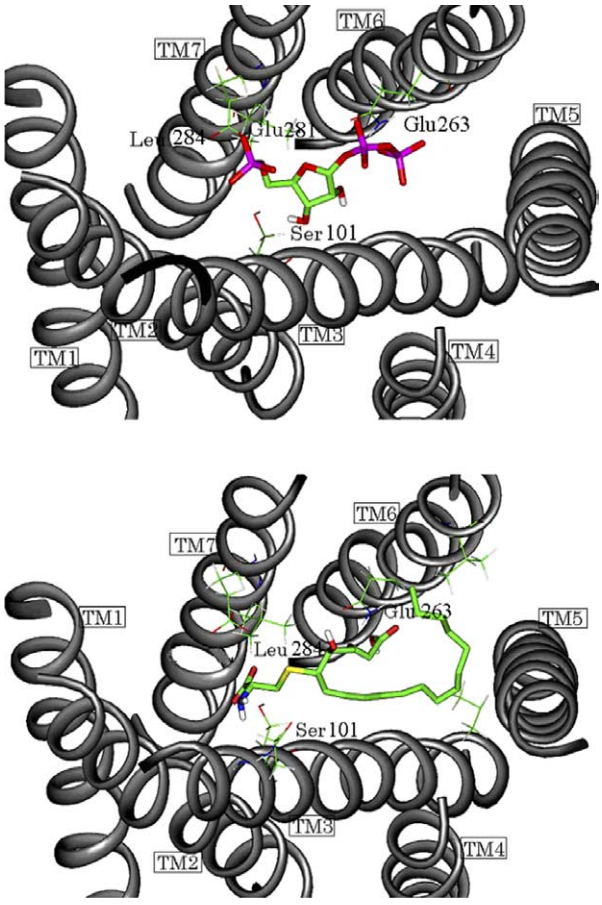

Fig. 4. 3D models of ligand-bound hP2Y$_{12}$ receptor. The side chains of the important residues in proximity to the docked PRPP (upper) and LTE4 (bottom) molecules are highlighted and labeled.

the ribose by TM3 (Fig. 4). Similar results were seen in the P2Y$_1$–PRPP complex [5].

Moreover, according to the model of P2Y$_{12}$ receptor–CysLTE4 complex (Fig. 4, bottom), 1-carboxylic acid and the 5-hydroxyl group of CysLTE4 were shown to interact with Glu263 of TM6, the amino acid portion of cysteinyl group interacts with Leu284 of TM7, and the carboxylic acid with Ser101 of TM3. These results suggested that CysLTE4 was also anchored by TM3, 6, and 7.

Using ClustalX, the amino acid sequences of 169 GPCRs were aligned and a phylogenetic tree was prepared. This phylogenetic analysis showed that CysLT-1 and -2 receptors were close to the P2Y-related receptor family that consists of 17 receptors. Interestingly, three orphan receptors, GPR87, GPR91, and GPR92, were placed in the P2Y-related family. These 17 sequences and leukotrieneB4 receptor sequences (shown as P2Y$_7$ and BLT2) were aligned, and the evolutionary relationships of the CysLT receptors to the P2Y receptors were analyzed by using neighbor joining with bootstrap steps (Fig. 5). The GPRC5B receptor, which belongs to the GPCR family B, was added as a root of a phylogenic tree and referred to as the out group.

As shown in Fig. 5, the P2Y-related family forms three subgroups: (i) P2Y$_{1,2,4,6,11,15}$ and GPR91 (labeled as P2Y$_1$-group), (ii) P2Y$_{12,13,14}$, GPR87, and CysLT1,2 (labeled as P2Y$_{12}$-group), and (iii) P2Y$_{5,8,9}$ and GPR92 (Fig. 5). CysLT-1 and -2 receptors were shown to belong to the P2Y$_{12}$-group, while P2Y$_7$ receptor was not in the P2Y-related family. In fact, the cDNA coding P2Y$_7$ receptor was cloned by homology cloning using P2Y$_1$ receptor gene as a probe. However, it has been renamed as a LTB4 receptor, since it is activated by LTB4 but not by nucleotides [20].

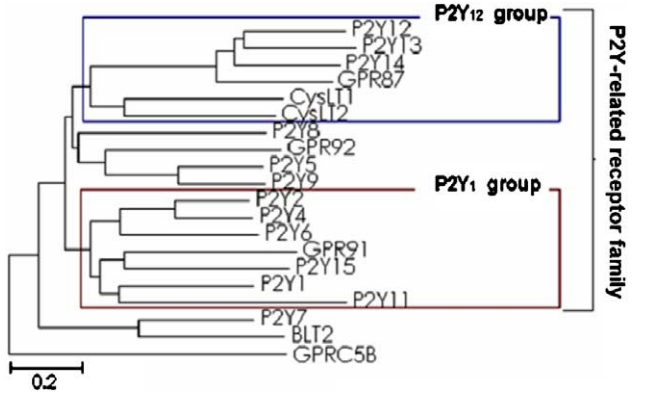

Fig. 5. Phylogenetic tree of the P2Y-related receptor family. Phylogenetic analysis was performed based on the neighbor-joining method. The scale bar indicates a maximum likelihood branch of 0.2 inferred substitutions per site.

By verifying the correlation of the P2Y$_{12}$-group and CysLT receptors, we have analyzed the sequences and found tentative motifs common to the six receptors in the P2Y$_{12}$-group (–P(F/L)(K/R)– in TM2, –M/L– in TM3, –FF-(C/S)F– in TM6, and –TL-L—C-(D/N)P– in TM7, Fig. 6). These motifs were not seen in any other P2Y receptors.

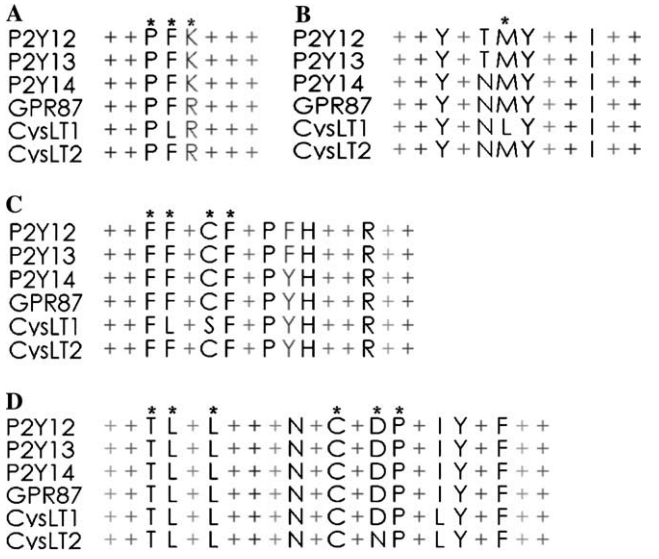

Fig. 6. The tentative motifs common to the P2Y$_{12,13,14}$, GPR87, and CysLT receptors (A); TM2 region near the extracellular site (B); TM3 region near the extracellular site (C); TM6 region in the middle of the transmembrane (D); whole region of TM7 * indicates the peculiar motifs not seen in other GPCRs.

Discussion

GPCRs are integral membrane proteins and interact with endogenous ligands such as neurotransmitters and hormones. Takeda et al. [21] have analyzed the human genome sequences using SOSUI and have reported that about 950 kinds of GPCRs exist on the human genome. GPCRs are known to be the action sites of more than half of all contemporary medicines. However, since the membrane protein does not readily crystallize, very few of the tertiary structures of GPCRs have been clarified. On the other hand, since the late 1990s, in silico methods have been considered to be strong strategies for drug screening and design. Thus, we tried to develop an in silico method to discover a novel surrogate ligand that interacts with the $P2Y_{12}$ receptor, a kind of GPCR.

Prior to in silico screening, a receptor assay for the $P2Y_{12}$ receptor was established. Empirically we know that various $P2Y_n$ ($n = 1,2,4,\ldots,14$) receptors are expressed in almost all cell lines. Therefore, we needed to develop an assay for $P2Y_{12}$ receptor that can distinguish $P2Y_{12}$ reaction from the reaction caused through the endogenous $P2Y_n$ receptors. Moreover, since the quantity of the endogenous G proteins is inadequate to interact with the highly expressed GPCRs in the host cells, it is necessary to increase the level of G proteins to a level similar to that of the expressed GPCR [22]. Although the $P2Y_{12}$ receptor intrinsically couples with G_i protein, which mainly controls the activity of adenylatecyclase but not phospholipase C (PLC), we prepared the $hP2Y_{12}$–$hG_{16}\alpha$ fusion proteins, because $G_{16}\alpha$ protein was reported to be universally coupled with many kinds of GPCRs, and its activation leads to stimulation of PLC leading to increase in the $[Ca^{2+}]_i$ that is easily measured [23,24].

When the $P2Y_1$ agonist, 2MeSADP, was perfused over the cells stably expressing the $P2Y_1$–$G_q\alpha$ or $P2Y_1$–$G_{16}\alpha$ proteins, the transient increases in $[Ca^{2+}]_i$ were obtained with EC_{50} values of 0.16 and 0.060 nM, respectively (Fig. 1). On the other hand, the EC_{50} value was 4.7 nM when using the wild type cells. Thus, we confirmed that the $P2Y_1$–$G_{16}\alpha$ fusion receptor functionally worked. The subsequent Ca^{2+} assay revealed that $hP2Y_{12}$–$hG_{16}\alpha$ was activated by 2MeSADP with the EC_{50} value of 0.059 nM, similar to that obtained with the $P2Y_1$–$G_{16}\alpha$ cells (Fig. 1). However, an EC_{50} value for $P2Y_{12}$–$G_i\alpha$ was 2.0 nM (Fig. 1). From these results, we concluded that the activation of $hP2Y_{12}$–$hG_{16}\alpha$ proteins could efficiently stimulate intracellular PLC activity.

The 3D structure of bovine rhodopsin suggested GPCRs possessed a ligand binding site in the membrane surface surrounded by seven transmembrane α-helices [25,26]. However, some of the seven α-helices have irregular bends. Moreover, the intrinsic ligand, retinol, is covalently bound to Lys in TM3 [25]. It is not expected that these features of transmembrane helices are always common to other GPCRs. We therefore have developed a method of modeling GPCRs by using straight helices of which seven regions were predicted by Fourier transform analysis, and imposing these helices to the rhodopsin structure by calculating root mean square deviation [5]. Using the newly constructed 3D model of the $P2Y_{12}$ receptor, the in silico screening selected PRPP and five CysLTs in addition to 20 nucleotides such as 2MeSADP, ADP, and ATP.

PRPP, which is a surrogate $P2Y_1$ agonist that was recently discovered by Hiramoto et al., induced the $[Ca^{2+}]_i$ increase in the $hP2Y_{12}$–$hG_{16}\alpha$ cells in a dose-dependent manner (Fig. 2). The EC_{50} value was 4.6 nM, much smaller than the value of 530 nM obtained with the wild type cells. The PRPP-induced $[Ca^{2+}]_i$ increase in the $hP2Y_{12}$–$hG_{16}\alpha$ cells was blocked by the $P2Y_{12}$ antagonist, 2MeSAMP. These results clearly showed that PRPP acted as an agonist not only on the $P2Y_1$ receptor but also on the $P2Y_{12}$ receptor. As shown in Fig. 3, CysLTE4 also stimulated the $P2Y_{12}$ receptor in a high affinity manner so that it induced a transient increase in $[Ca^{2+}]_i$. The increase was prevented by 2MeSAMP, suggesting that CysLTE4 acted on the $P2Y_{12}$ receptor as a full agonist.

The 3D models of $P2Y_{12}$–PRPP and $P2Y_{12}$–CysLTE4 complexes indicated that the interactions of these agonists were carried out by TM3, TM6, and TM7 (Fig. 4). These interactions can be seen in the $P2Y_1$–ligand complexes in which PRPP and ADP interacted with TM3, 6, and 7 [5]. On the other hand, the $P2Y_1$ antagonists, PPADS and adenosine3′,5′ bisphosphate, were shown to interact with TM4, TM5, TM6, and TM7. These different binding manners may cause functional differences in receptor activation.

Although the $P2Y_{12}$ antagonists, ticlopidine and clopidogrel, are used for the medical treatment of thrombosis, aspirin is required for a more effective treatment. On the contrary, it is known that thrombogenesis increases with aspirin for some patients [27,28]. The reason aspirin is often prescribed as a thrombosis treatment is that it is considered to have an inhibitory effect on the cyclo-oxygenase activity in the arachidonate cascade. That is, thrombogenesis is suppressed by reducing the production of TXA2 from arachidonate. However, administration of aspirin increases free arachidonic acid which leads to the accumulation of leukotrienes that are usually metabolized by 5-lipoxygenase from arachidonic acid. CysLTE4 has been known to activate the CysLT receptors as a slow-reacting substance of anaphylaxis [29,30]. In addition, CysLTE4 was reported to accelerate thrombosis by an unknown mechanism [16]. In the present study, we found that CysLTE4 acted as an endogenous agonist on the $P2Y_{12}$ receptor. These results suggest that the increase in thrombogenesis by aspirin can be partially explained by the result of the accumulation of CysLTE4, which activates the $P2Y_{12}$ receptor on the platelets.

Nowadays, an antagonist reversibly as well as directly acting on both $P2Y_1$ and $P2Y_{12}$ receptors is strongly anticipated as a new efficient thrombosis treatment [12,13]. In the present study, we found PRPP activated both $P2Y_1$–$G_{16}\alpha$ and $P2Y_{12}$–$G_{16}\alpha$ fusion receptors with high affinity. Moreover,

PRPP induced rabbit platelet aggregation in a dose-dependent manner and the PRPP-induced aggregation was blocked by 2MeSAMP as well as PPADS (Environmental Biological Life Science Research Center, Shiga, personal communication). Therefore, PRPP may provide a basic frame to develop a thrombogenesis inhibitor.

Phylogenetic analysis of the P2Y, P2Y-like orphan, and CysLT receptors showed that CysLT receptors had a close relationship to the P2Y-related family. Furthermore, the analysis suggested that the P2Y-related family can be divided into three subgroups; $P2Y_1$-group ($P2Y_{1,2,4,6,11,15}$ and GPR91), $P2Y_{12}$-group ($P2Y_{12,13,14}$, GPR87, and CysLT1,2), and others ($P2Y_{5,8,9}$ and GPR92) (Fig. 5).

While $P2Y_1$ and $P2Y_2$ receptors interact with ADP and UTP with the EC_{50} values of $10^{-7\sim-8}$ and$10^{-5\sim-7}$ M, respectively [5,31,32], these receptors did not show any response to 10^{-6} M CysLTC4, CysLTD4 or CysLTE4 (data not shown). The CysLT receptors interact in a high affinity manner with CysLTs ($EC_{50} = 10^{-7\sim9}$ M) as well as UDP ($EC_{50} = 10^{-7\sim9}$ M) [29,30]. As shown here, the $P2Y_{12}$ receptor also interacts with both nucleotides and CysLTE4 in a high affinity manner. Thus, we assume that the receptors in the $P2Y_1$-group interact with only nucleotides, whereas the receptors in the $P2Y_{12}$-group interact with both nucleotides and CysLTs. Joost and Methner [33] have predicted that UDP-glucose was a ligand for GPR87. According to our phylogenetic analyses, GPR87 belongs to the $P2Y_{12}$-group and possesses the tentative motifs seen only in the $P2Y_{12}$-group (Fig. 6). Therefore, we support their proposal and moreover we predict that GPR87 can be activated not only by nucleotides but also by CysLTs. The tentative motifs presented in TM2, TM3, TM6, and TM7 in the $P2Y_{12}$-group should be further investigated to see if they play important roles for a common function in intramolecular signal transduction.

Acknowledgment

We thank Dr. E. Cooper in Ritsumeikan University for help in preparing the manuscript.

Appendix A. Supplementary data

Supplementary data associated with this article can be found, in the online version, at doi:10.1016/j.bbrc.2005.09.052.

References

[1] International Human Genome Sequencing Consortium, Finishing the euchromatic sequence of the human genome, Nature 431 (2004) 931–945.
[2] F.S. Collins, E.D. Green, A.E. Guttmacher, M.S. Guyer, A vision for the future of genomics research, Nature 422 (2003) 835–847.
[3] G. Muller, Towards 3D structures of G protein-coupled receptors: multidisciplinary approach, Curr. Med. Chem. 7 (2000) 861–888.
[4] K. Gohda, I. Mori, D. Ohta, T. Kikuchi, ACoMFA analysis with conformational propensity: an attempt to analyze the SAR of a set of molecules with different conformational flexibility using a 3D-QSAR method, J. Comput. Aid. Mol. Des. 14 (2000) 265–275.
[5] T. Hiramoto, Y. Nonaka, K. Inoue, T. Yamamoto, M. Omatsu-Kanbe, H. Matsuura, K. Gohda, N. Fujita, Identification of endogenous surrogate ligands for human P2Y receptors through an in silico search, J. Pharmacol. Sci. 95 (2004) 81–93.
[6] T. Hiramoto, W. Nemoto, T. Imai, T. Kikuchi, N. Fujita, Construction of hypothetical three-dimensional structure of $P2Y_1$ receptor based on Fourier transform analysis, J. Protein Chem. 8 (2002) 537–545.
[7] G.M. Morris, D.S. Goodsell, R. Huey, A.J. Olson, Distributed automated docking of flexible ligands to proteins: parallel applications of AutoDock 2.4, J. Comput. Aid. Mol. Des. 4 (1996) 293–304.
[8] M. Kanehisa, S. Goto, S. Kawashima, Y. Okuno, M. Hattori, The KEGG resource for deciphering the genome, Nucleic Acids Res. 32 (2004) D277–D280.
[9] M.P. Abbracchio, J.M. Boeynaems, E.A. Barnard, J.L. Boyer, C. Kennedy, M.T. Miras-Portugal, B.F. King, C. Gachet, K.A. Jacobson, A. Weisman, G. Burnstock, Characterization of the UDP-glucose receptor (re-named here the $P2Y_{14}$ receptor) adds diversity to the P2Y receptor family, Trends Pharmacol. Sci. 24 (2003) 52–55.
[10] T. Wittenberger, H. Schaller, S. Hellebrands, An expressed sequence tag (EST) data mining strategy succeeding in the discovery of new G-protein coupled receptors, J. Mol. Biol. 307 (3) (2001) 799–813.
[11] G. Hollopeter, H.M. Jantzen, D. Vincent, G. Li, L. England, V. Ramakrishnan, R.B. Yang, P. Nurden, A. Nurden, D. Julius, P.B. Conley, Identification of the platelet ADP receptor targeted by antithrombotic drugs, Nature 409 (2001) 202–207.
[12] R.T. Dorsam, S.P. Kunaupli, Central role of the $P2Y_{12}$ receptor in platelet activation, J. Clin. Invest. 133 (2004) 340–345.
[13] J.C. Resendiz, S. Feng, G. Ji, K.A. Francis, M.C. Berndt, M.H. Kroll, Purinergic $P2Y_{12}$ receptor blockade inhibits shear-induced platelet phosphatidylinositol 3-kinase activation, Mol. Pharmacol. 63 (2003) 639–645.
[14] M. Radomski, The biological role of thromboxane A2 in the process of hemostasis and thrombosis; pharmacology and perspectives of therapeutical use of thromboxane synthetase inhibitors and receptor PGH2/TXA2 antagonists, Acta Physiol. Pol. 36 (3) (1985) 153–164.
[15] L. Macchia, M. Hamberg, M. Kumlin, J.H. Butterfield, J.Z. Haeggstrom, Arachidonic acid metabolism in the human mast cell line HMC-1: 5-lipoxygenase gene expression and biosynthesis of thromboxane, Biochim. Biophys. Acta 1257 (1995) 58–74.
[16] J.L. Mehta, W.W. Nichols, Leukotriene-receptor antagonist FPL-55712 and t-PA-induced thrombolysis in canine coronary thrombosis, Thromb. Res. 58 (1) (1990) 13–21.
[17] I. Weide, M. Winking, T. Simmet, Intravascular cysteinyl–leukotriene formation by clotting whole human blood. Evidence from clamped umbilical vein segments and thrombus specimens, Thromb. Res. 72 (1) (1993) 83–90.
[18] S. Kumar, K. Tamura, M. Nei, Integrated software for molecular evolutionary genetics analysis and sequence alignment, Bioinformatics 5 (2004) 150–163.
[19] B. Marcet, V. Chappe, P. Delmas, B. Verrier, Pharmacological and signaling properties of endogenous $P2Y_1$ receptors in cystic fibrosis transmembrane conductance regulator-expressing Chinese hamster ovary cells, J. Pharmacol. Exp. Ther. 309 (2) (2004) 533–539.
[20] T. Yokomizo, T. Izumi, K. Chang, Y. Takuwa, T. Shimizu, A G-protein-coupled receptor for leukotriene B4 that mediates chemotaxis, Nature 387 (1997) 620–624.
[21] S. Takeda, S. Kadowaki, T. Haga, H. Takaesu, S. Mitaku, Identification of G protein-coupled receptor genes from the human genome sequence, FEBS Lett. 520 (2002) 97–101.
[22] Z.D. Guo, H. Suga, M. Okamura, S. Takeda, T. Haga, Receptor-Gα fusion proteins as a tool for ligand screening, Life Sci. 68 (2001) 2319–2327.

[23] S. Offermanns, M.I. Simon, G alpha 15 and G alpha 16 couple a wide variety of receptors to phospholipase C, J. Biol. Chem. 270 (1995) 15175–15180.
[24] H. Suga, S. Takeda, T. Haga, M. Okamura, K. Takao, K. Tatemoto, Stimulation of increases in intracellular calcium and prostaglandin E2 generation in Chinese hamster ovary cells expressing receptor-Galpha 6 fusion proteins, J. Biochem. (Tokyo) 135 (5) (2004) 605–613.
[25] K. Palczewski, T. Kumasaka, T. Hori, C.A. Behnke, H. Motoshima, B.A. Fox, I. Le Trong, D.C. Teller, T. Okada, R.E. Stenkamp, M. Yamamoto, M. Miyano, Crystal structure of rhodopsin: a G protein-coupled receptor, Science 289 (2000) 739–745.
[26] T. Okada, Y. Fujiyoshi, M. Silow, J. Navarro, E.M. Landau, Y. Shichida, Functional role of internal water molecules in rhodopsin revealed by x-ray crystallography, Proc. Natl. Acad. Sci. USA 99 (2002) 5982–5987.
[27] H. Neubauer, B. Gunesdogan, C. Hanefeld, M. Spiecker, A. Mugge, Lipophilic statins interfere with the inhibitory effects of clopidogrel on platelet function—a flow cytometry study, Eur. Heart J. 24 (19) (2003) 1744–1749.
[28] R. Grossmann, O. Sokolova, A. Schnurr, A. Bonz, C. Porsche, A. Obergfell, B. Lengenfelder, U. Walter, M. Eigenthaler, Variable extent of clopidogrel responsiveness in patients after coronary stenting, Thromb. Haemost. 92 (6) (2004) 1201–1206.
[29] H.M. Sarau, R.S. Ames, J. Chambers, C. Ellis, N. Elshourbagy, J.J. Foley, D.B. Schmidt, R.M. Muccitelli, O. Jenkins, P.R. Murdock, N. Herrity, W. Halsey, G. Sathe, A.I. Muir, P. Nuthulaganti, G.M. Dytko, P.T. Buckley, S. Wilson, D.J. Bergsma, D.W. Hay, Identification, molecular cloning, expression, and characterization of a cysteinyl leukotriene receptor, Mol. Pharmacol. 56 (1999) 657–663.
[30] C.E. Heise, B.F. O'Dowd, D.J. Figueroa, N. Sawyer, T. Nguyen, D.S. Im, R. Stocco, J.N. Bellefeuille, M. Abramovitz, R. Cheng, D.L. Williams Jr., Z. Zeng, Q. Liu, L. Ma, M.K. Clements, J.F. Evans, Characterization of the human cysteinyl leukotriene 2 receptor, J. Biol. Chem. 275 (2000) 30531–30536.
[31] J. Simon, A.K. Filippov, S. Goransson, Y.H. Wong, C. Frelin, A.D. Michel, D.A. Brown, E.A. Barnard, Characterization and cannel coupling of the $P2Y_{12}$ nucleotide receptor of brain capillary endothelial cells, J. Biol. Chem. 277 (2002) 31390–31400.
[32] L.L. Clarke, M.C. Harline, M.A. Otero, G.G. Glover, R.C. Garrad, B. Krugh, N.M. Walker, F.A. Gonzalez, J.T. Turner, G.A. Weisman, Desensitization of $P2Y_2$ receptor-activated transepithelial anion secretion, Am. J. Physiol. 276 (4 Pt. 1) (1999) C777–C787.
[33] P. Joost, A. Methner, Phylogenetic analysis of 277 human G protein-coupled receptors as a tool for the prediction of orphan receptor ligands, Genome Biol. 3 (11) (2002) 1–16.